Optics Communications 550 (2024) 129933

Contents lists available at ScienceDirect

Optics Communications

journal homepage: www.elsevier.com/locate/optcom

Analytical analysis of the beam propagation factor of elegant Hermite-Gaussian and elegant Laguerre-Gaussian beams with astigmatism

Chemist M. Mabena

CSIR Photonics Centre, Meiring Naudé Road, Pretoria, 0001, Gauteng, South Africa

ARTICLE INFO

Keywords:
Elegant Hermite–Gaussian beams
Elegant Laguerre–Gaussian beams
Beam propagation factor
Astigmatism
Phase aberrations

ABSTRACT

The impact of astigmatism on the beam propagation factor (M^2) of elegant Hermite–Gaussian and elegant Laguerre–Gaussian beams is examined. We derive closed-form expressions for M^2 when the optical beams are aberrated with astigmatism. The analysis shows that the beam radius is crucial to the degree of impact astigmatism has on M^2. To this extent, we derive the beam radius that separates the region where the M^2 is negligibly affected and the region where it becomes severely affected. For the elegant Laguerre-Gaussian beams, we establish a parameter that determines a set of beams that are impacted equally by astigmatism. The analytical results are validated with numerical simulations.

1. Introduction

Hermite-Gaussian and Laguerre-Gaussian beams are eigenmodes of the paraxial wave equation in cartesian and cylindrical symmetry, respectively. Their orthonormality and completeness make them a suitable basis choice for optical resonator modes and propagating optical beams. In addition to being an ideal basis set, these higher-order Gaussian laser beams have received considerable attention within the optics community and have found applications in various fields such as optical trapping [1,2], free-space communication [3–5], and quantum optics [6–8]. While the conventional high-order Gaussian beams have amassed a lot of attention, there exists a different set of modes of the paraxial wave equation, which are also becoming topical, called the elegant Hermite-Gaussian and elegant Laguerre-Gaussian (eHG and eLG) beams. They are defined in the same way as the conventional Hermite-Gaussian and Laguerre–Gaussian beams except that the polynomial functions have complex arguments. The complex arguments create a symmetry between the polynomial functions and the Gaussian envelop, which is the origin of the elegant description in their name. A notable physical property of the elegant Gaussian beams is that their transverse intensity distribution does not remain constant during propagation [9]. A venerable body of work has been done toward understanding their propagation properties [9–19]. Furthermore, elegant Gaussian beams have been reported as a promising alternative to standard high-order Gaussian beams in applications such as optical manipulation [20].

The beam propagation factor (M^2) is a critical parameter that can be used to quantify the quality of a laser beam [21–28]. It gives information about the propagation dynamics of the laser beam such as how tightly it will focus or how much it will diverge upon propagation. Saghafi and Sheppard performed calculations for the beam propagation factor of higher-order elegant Gaussian beams in an aberration-free optical system [10]. They obtained an analytical expression for the beam propagation factor of the elegant Hermite-Gaussian beams and an expression for elegant Laguerre-Gaussian beams only in the special case of $|\ell| = 0$. A simplified expression for the beam propagation factor of elegant Laguerre-Gaussian beams was derived for the first time in the work by Porras et al. [29]. Some work has been done to understand the behavior of elegant Gaussian beams in truncated systems. Zhao and Mei [19] derived a generalized beam propagation factor expression of truncated elegant Laguerre-Gaussian beams. In a more recent study, an analytical expression for the beam propagation factor of 1D truncated elegant Hermite-Gaussian beams was derived by Mihoubi et al. [30]. The effect of atmospheric turbulence [16,31,32] and misaligned systems [13,33] on elegant Gaussian beams has also been investigated.

It is generally accepted that optical elements or systems are not ideal and may contain aberrations. A phase aberration can be represented as a complex function that modifies the wavefront of a laser beam. Phase aberrations can be introduced into an optical system as a result of misalignment, in optical elements due to manufacturing imperfections or thermal effects [34]. Astigmatism is one of the most common aberrations that occur in optical systems. The presence of astigmatism in an optical system leads to a degradation of the quality of the laser beam that traverses the system. In order to inform the design and development of laser systems that are dominated by astigmatism, it is useful to know and quantify the amount of degradation it can cause.

E-mail address: mabenacm@gmail.com.

https://doi.org/10.1016/j.optcom.2023.129933
Received 2 August 2023; Received in revised form 5 September 2023; Accepted 9 September 2023
Available online 16 September 2023

In this work, we use the method of moments and the generation functions of elegant Hermite-Gaussian and elegant Laguerre-Gaussian beams to derive compact and simplified analytical expressions for the beam propagation factor due to astigmatism. While a venerable body of work exists on the experimental measurement of the beam propagation factor, analytical methods, and expressions remain essential to understanding quantitative and qualitative features, especially when parametric studies are to be done or when expeditious results are required. This work contributes to the body of knowledge on the understanding of elegant Gaussian beams and the design of optical systems that use elegant Gaussian beams.

2. Elegant Gaussian beams

2.1. Elegant Hermite-Gaussian beams

The elegant Hermite-Gaussian (eHG) beams are solutions of the paraxial wave equation and have a complex amplitude that is expressible as follows,

$$\mathrm{eHG}(x,y,z) = \left(\frac{q_0}{q(z)}\right)^{\frac{n+m}{2}+1} \mathcal{H}_n\left(\sqrt{\frac{ik}{2q(z)}}x\right)\mathcal{H}_m\left(\sqrt{\frac{ik}{2q(z)}}y\right) \times \exp\left[-\frac{ik}{2q(z)}\left(x^2+y^2\right) - ikz\right], \tag{1}$$

where $q(z) = 1/\left(\frac{1}{R(z)} + \frac{i\lambda}{\pi\omega^2(z)}\right)$ is the complex beam parameter, $q_0 = q(0)$, the wavefront curvature is given as $R(z) = z + \frac{z_R^2}{z}$, beam radius as a function of propagation distance $\omega^2(z) = \omega_0^2\left(1+\frac{z^2}{z_R^2}\right)$, with the Rayleigh range is expressed as $z_R = \frac{\pi\omega_0^2}{\lambda}$ where ω_0 is the beam radius of the Gaussian beam envelope at the waist, λ is the wavelength of the eHG laser beam, $k = 2\pi/\lambda$, $H_n(\cdot)$ and $H_m(\cdot)$ are the Hermite polynomials. At the waist, the eHG complex amplitude can be expressed in terms of a generating function as follows,

$$\mathcal{H} = \exp\left[\frac{2x\mu}{\omega_0} + \frac{2y\eta}{\omega_0} - \left(\mu^2+\eta^2\right) - \frac{\left(x^2+y^2\right)}{\omega_0^2}\right], \tag{2}$$

where μ and η are the generating parameters for the n and m indices, respectively. To generate a particular eHG expression, one has to perform the differentiation as follows,

$$\mathrm{eHG}_{n,m} = \frac{1}{\mathcal{N}_{\mathrm{eHG}}}\left[\frac{\partial^m}{\partial\eta^m}\frac{\partial^n}{\partial\mu^n}\mathcal{H}\right]_{\eta,\mu=0}, \tag{3}$$

where $\mathcal{N}_{\mathrm{eHG}}$ is a normalization constant given by,

$$\mathcal{N}_{\mathrm{eHG}} = \left[\frac{\partial^m}{\partial\eta_1^m}\frac{\partial^m}{\partial\eta_2^m}\frac{\partial^n}{\partial\mu_1^n}\frac{\partial^n}{\partial\mu_2^n}\mathcal{N}\right]_{\eta_1,\eta_2,\mu_1,\mu_2=0} \tag{4}$$

with $\mathcal{N}$ given as follows,

$$\mathcal{N} = \sqrt{\frac{2\exp\left[\frac{\eta_1^2+\eta_2^2}{2} - \eta_1\eta_2 + \frac{(\mu_1-\mu_2)^2}{2}\right]}{\pi\omega_0^2}}. \tag{5}$$

Examples of the intensity profiles of selected eHG laser beams together with their respective phases are shown in Fig. 1.

2.2. Elegant Laguerre-Gaussian beams

The elegant Laguerre-Gaussian (eLG) beams are also solutions of the paraxial wave equation, albeit in cylindrical coordinates. Their complex amplitude is expressible as follows,

$$\mathrm{eLG}(r,\phi,z) = \left(\frac{q_0}{q(z)}\right)^{\frac{p+|\ell|}{2}+1}\mathcal{L}_p^{|\ell|}\left(\frac{i\pi}{\lambda q(z)}r^2\right) \times \exp\left[-\frac{i\pi}{\lambda q(z)}r^2 - ikz\right]\exp\left[i\ell\phi\right], \tag{6}$$

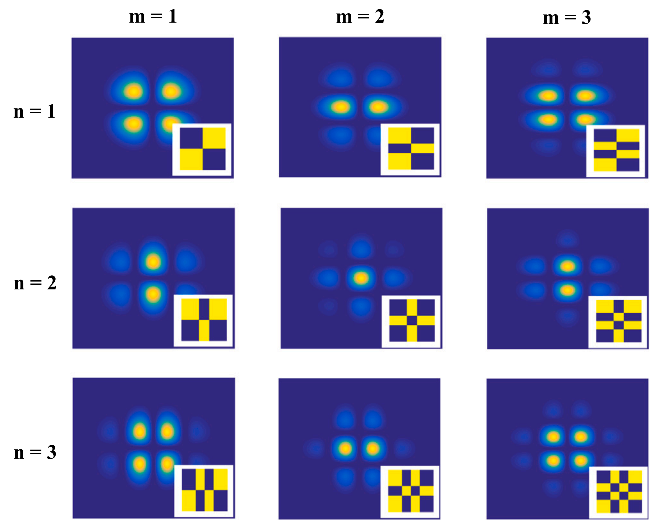

Fig. 1. Intensity cross-section of selected eHG laser beams at the waist plane. The insets at the bottom right corner show the phase of each optical beam.

where $\mathcal{L}_p^{|\ell|}$ is the generalized Laguerre polynomial, ℓ and p are the azimuthal and radial indices, respectively, $\phi = \arctan\left(\frac{y}{x}\right)$, and all the other terms are similar to those defined in Section 2.1.

At the waist plane, the eLG complex amplitude can be expressed in terms of a generating function, in cartesian coordinates, as follows,

$$\mathcal{G} = \frac{1}{1-\eta}\exp\left[\frac{(x+i\mathrm{T}y)\mu}{\omega_0(1-\eta)} - \frac{\left(x^2+y^2\right)\eta}{\omega_0^2(1-\eta)} - \frac{\left(x^2+y^2\right)}{\omega_0^2}\right], \tag{7}$$

where μ and η are the generating parameters for the azimuthal (ℓ) and radial (p) indices, respectively,and T gives the sign of the azimuthal index ℓ. To generate a particular eLG, one has to perform the differentiation as follows,

$$\mathrm{eLG}_{\ell,p} = \frac{1}{\mathcal{N}_{\mathrm{eLG}}}\left[\frac{\partial^p}{\partial\eta^p}\frac{\partial^{|\ell|}}{\partial\mu^{|\ell|}}\mathcal{G}\right]_{\eta,\mu=0}, \tag{8}$$

where $\mathcal{N}_{\mathrm{eLG}}$ is a normalization constant given by,

$$\mathcal{N}_{\mathrm{eLG}} = \left[\frac{\partial^p}{\partial\eta_1^p}\frac{\partial^p}{\partial\eta_2^p}\frac{\partial^{|\ell|}}{\partial\mu_1^{|\ell|}}\frac{\partial^{|\ell|}}{\partial\mu_2^{|\ell|}}\mathcal{N}\right]_{\eta_1,\eta_2,\mu_1,\mu_2=0} \tag{9}$$

with $\mathcal{N}$ given as follows,

$$\mathcal{N} = \sqrt{\frac{\pi\omega_0^2\exp\left[\frac{\mu_1\mu_2}{2-\eta_1-\eta_2}\right]}{2-\eta_1-\eta_2}}. \tag{10}$$

Examples of the intensity profiles of selected eLG laser beams together with their respective phases are shown in Fig. 2.

3. Beam propagation factor

The beam propagation factor is invariant when passing through an ideal optical system, a linear system, or when passing through a system with a quadratic transfer function such as a lens. Real optical systems have aberrations and the presence of aberrations degrades the quality of the laser beams. Here, we will use the method of moments to calculate the beam propagation factor, which is a critical parameter that is used in practice to characterize the quality of a laser beam. If we assume that the propagation of the laser beam along the two axes can be treated as independent, the beam propagation factor along the x and y directions is given as follows,

$$M_x^2 = 4\pi\sqrt{\langle x^2\rangle\langle\theta_x^2\rangle - \langle x\theta_x\rangle^2}, \tag{11}$$

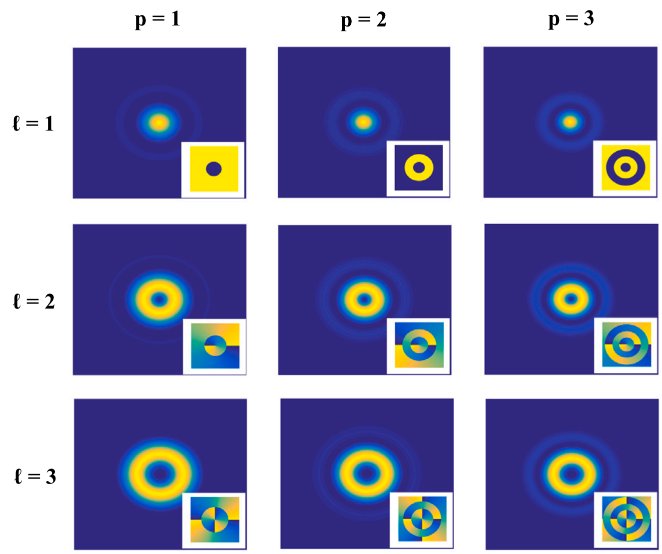

Fig. 2. Intensity cross-section of selected eLG laser beams at the waist plane. The insets at the bottom right corner show the phase of each laser beam.

$$M_y^2 = 4\pi\sqrt{\langle y^2\rangle\langle\theta_y^2\rangle - \langle y\theta_y\rangle^2}, \tag{12}$$

where $\langle x^2\rangle$ and $\langle y^2\rangle$ are the second-order spatial moments along the x and y directions, respectively; $\langle\theta_x^2\rangle$ and $\langle\theta_y^2\rangle$ are the second-order angular moments in each direction; $\langle x\theta_x\rangle$ and $\langle y\theta_y\rangle$ are the first-order spatial-angular moments in the x and y directions, respectively. The terms represented in Eq. (11) can be calculated as follows,

$$\langle x^2\rangle = \int_{-\infty}^{\infty}\int_{-\infty}^{\infty} x^2u^2(x,y)\,dxdy, \tag{13}$$

$$\langle\theta_x^2\rangle = \frac{1}{4\pi^2}\int_{-\infty}^{\infty}\int_{-\infty}^{\infty}\left[\left(\frac{\partial u}{\partial x}\right)^2 + \left(u\frac{\partial\phi}{\partial x}\right)^2\right]dxdy - \frac{1}{4\pi^2}\left(\int_{-\infty}^{\infty}\int_{-\infty}^{\infty}u^2\frac{\partial\phi}{\partial x}dxdy\right)^2, \tag{14}$$

For convenience, we break up Eq. (14) into three different parts as follows: the first term does contain any aberration information,

$$\theta_1 = \frac{1}{4\pi^2}\int_{-\infty}^{\infty}\int_{-\infty}^{\infty}\left(\frac{\partial u}{\partial x}\right)^2 dxdy, \tag{15}$$

the aberration-dependent terms are given as,

$$\theta_2 = \frac{1}{4\pi^2}\int_{-\infty}^{\infty}\int_{-\infty}^{\infty}\left(u\frac{\partial\phi}{\partial x}\right)^2 dxdy, \tag{16}$$

and,

$$\theta_3 = \frac{1}{2\pi}\int_{-\infty}^{\infty}\int_{-\infty}^{\infty}u^2\frac{\partial\phi}{\partial x}dxdy. \tag{17}$$

With this, the second-order angular moment can be rewritten as follows,

$$\langle\theta_x^2\rangle = \theta_1 + \theta_2 - \theta_3^2. \tag{18}$$

Finally, from Eq. (11) we also have the first-order spatial-angular moment, which is calculated as follows,

$$\langle x\theta_x\rangle = \frac{1}{2\pi}\int_{-\infty}^{\infty}\int_{-\infty}^{\infty}u^2x\frac{\partial\phi}{\partial x}dxdy. \tag{19}$$

The terms in Eq. (12) are given by the same formulae as above, albeit with the appropriate substitution of the x and y variables.

Table 1
Algebraic expressions for primary astigmatism.

Description	Algebraic expression
0° astigmatism	$D_{\text{ast0}}\left(x^2 - y^2\right)$
45° astigmatism	$D_{\text{ast45}}xy$

The complex amplitude of a laser beam can be expressed as follows,

$$E(x,y) = u(x,y)e^{-i\frac{2\pi}{\lambda}\phi(x,y)}, \tag{20}$$

where $u(x,y)$ is the complex amplitude distribution of the laser beam, $\phi(x,y)$ represents the phase accrued as a result of aberrations. Table 1 shows the algebraic expressions for the aberrations considered in this work. The coefficients D_{ast0} and D_{ast45} have units of diopter.

3.1. Beam propagation factor of aberrated elegant Hermite-Gaussian beams

3.1.1. 0° astigmatism

It can be easily shown that the beam propagation factor of eHG laser beams is not affected by 0° astigmatism. We can start by substituting the expression for 0° astigmatism (Table 1) into Eq. (16), which becomes the second-order spatial moment with an extra factor $\frac{1}{\pi^2}$. A similar substitution into Eq. (17) gives the first-order spatial moment, which is zero. Substitution of the expression for 0° astigmatism (Table 1) into Eq. (19) also results in the second-order spatial moment with an extra factor $\frac{1}{\pi}$. Putting everything together and substituting all of the above into Eq. (11) gives,

$$M_x^2 = 4\pi\sqrt{\langle x^2\rangle\theta_1}. \tag{21}$$

This shows that the beam propagation factor is unchanged by 0° astigmatism. This conclusion also holds for the case of eLG laser beams.

3.1.2. 45° astigmatism

The beam propagation factor of eHG laser beams is not unaffected by 45° astigmatism. The second-order spatial moment in terms of the generating parameters, is given as follows,

$$\langle x^2\rangle_{\text{eHG}} = \frac{\pi\omega_0^4\exp\left\{-\frac{\eta_1^2+\eta_2^2+(\mu_1-\mu_2)^2}{2}+\eta_1\eta_2\right\}\left[\left(\mu_1+\mu_2\right)^2+1\right]}{8\mathcal{N}_{\text{eHG}}^2}, \tag{22}$$

The aberration independent term in Eq. (18) for 45° astigmatism is given below as

$$\theta_{1,x}^{\text{ast45}} = \frac{\exp\left\{-\frac{\eta_1^2+\eta_2^2+(\mu_1-\mu_2)^2}{2}+\eta_1\eta_2\right\}\left[\mu_1-\mu_2+1\right]\left[\mu_1-\mu_2-1\right]}{8\pi\mathcal{N}_{\text{eHG}}^2}, \tag{23}$$

Next, we consider the aberration-dependent terms, which are given by,

$$\theta_{2,x}^{\text{ast45}} = \frac{D_{\text{ast45}}^2\omega_0^4\pi\exp\left\{-\frac{\eta_1^2+\eta_2^2+(\mu_1-\mu_2)^2}{2}+\eta_1\eta_2\right\}\left[\left(\eta_1+\eta_2\right)^2+1\right]}{\mathcal{N}_{\text{eHG}}^2 8\lambda^2}, \tag{24}$$

$$\theta_{3,x}^{\text{ast45}} = \frac{D_{\text{ast45}}\omega_0^3\pi\exp\left\{-\frac{\eta_1^2+\eta_2^2+(\mu_1-\mu_2)^2}{2}+\eta_1\eta_2\right\}\left[\eta_1+\eta_2\right]}{4\lambda\mathcal{N}_{\text{eHG}}^2}, \tag{25}$$

Finally, the expression for the first-order spatial-angular moment for 45° astigmatism in terms of generating parameters is given as,

$$\langle x\theta_x\rangle^{\text{ast45}} = \frac{D_{\text{ast45}}^2\omega_0^4\pi\exp\left\{-\frac{\eta_1^2+\eta_2^2+(\mu_1-\mu_2)^2}{2}+\eta_1\eta_2\right\}\left(\mu_1+\mu_2\right)\left(\eta_1+\eta_2\right)}{8\lambda\mathcal{N}_{\text{eHG}}^2}. \tag{26}$$

With the above expressions, the next step is to substitute them into Eq. (11) and carefully perform some calculations to obtain the beam propagation factor along the x directions as,

$$M_x^4 = \frac{\pi^2\omega_0^4 D^2_{\mathrm{ast45}}}{\lambda^2}\frac{(4m-1)(4n-1)}{(2m-1)(2n-1)} + \frac{(4n-1)(2n+1)}{2n-1}. \tag{27}$$

The expressions used to calculate the beam quality factor along the y direction are similar to those given in Eqs. (22) to (26), except for the terms in the square brackets. In this case, the generating parameters need to be replaced with the alternative. For instance, in Eq. (22) the following substitution has to be made: $\mu_1 \to \eta_1, \mu_2 \to \eta_2$. Using the same approach for the beam propagation factor along the y direction yields the following result,

$$M_y^4 = \frac{\pi^2\omega_0^4 D^2_{\mathrm{ast45}}}{\lambda^2}\frac{(4m-1)(4n-1)}{(2m-1)(2n-1)} + \frac{(4m-1)(2m+1)}{2m-1}. \tag{28}$$

Fig. 3 shows the beam propagation factor of various eHG optical beams aberrated by 45° astigmatism as a function of beam radius. The solid lines represent the beam quality factor for an aberration coefficient given by 0.01 cm^{-1} and the dashed lines represent an aberration coefficient of 1 cm^{-1}. The plots in Fig. 3 have a similar trend: the beam propagation factor is almost flat and changes infinitesimally up until a certain threshold beam radius. Beyond the threshold beam radius, the beam propagation factor starts changing sharply. We define the beam radius that separates these two regions as the critical width. The critical width depends on the n and m indices of the eHG beam, astigmatism strength, and the wavelength of the laser beam as follows,

$$\omega_c^{\mathrm{ast45}} = \left[\frac{\lambda^2}{\pi^2 D^2_{\mathrm{ast}}}\frac{(2m-1)(2n-1)}{(4m-1)(4n-1)}\right]^{\frac{1}{4}}. \tag{29}$$

For eHG laser beams with a beam radius that is larger than the critical width, $\omega_c \ll \omega_0$, the beam propagation factor, in both the x and y directions, can be approximated as a quadratic function in beam radius, ω_0, as follows,

$$M^2_{x,y} \simeq \frac{\pi\omega_0^2 D_{\mathrm{ast45}}}{\lambda}\sqrt{\frac{(4m-1)(4n-1)}{(2m-1)(2n-1)}}. \tag{30}$$

Since Fig. 3 is a log–log plot of the beam propagation factor versus beam radius, Eq. (30) appears as a straight line with a slope determined by the exponent of ω_0 and the y–intercept, for a fixed wavelength, is determined by the indices of the eHG laser beam and the strength of the 45° astigmatism. The beam propagation factor plots for different eHG laser beams cross each other due to the different critical widths. Some eHG laser beams pass their critical width while others have not and thus move into the region which is described by the straight line while the rest are still relatively flat. However, once all the beams pass their critical width, all the lines remain parallel, except for the laser beams for some cases where the beam propagation factor plots join. Looking at Eq. (30), it can be seen that the beam propagation factor in the region of sharp increase is symmetric about $m = n$. When two eHG optical beams are related by a swap of their indices, their beam propagation factors are exactly equal. For instance, eHG_{01} and eHG_{10} behave exactly the same in the region of sharp increase.

3.2. Beam propagation factor of aberrated elegant Laguerre-Gaussian beams

3.2.1. 45° astigmatism

Elegant Laguerre-Gaussian laser beams are symmetric, therefore, we expect the propagation dynamics along the $x-$ and $y-$ directions to be similar. With this, we only focus on Eq. (11). The second-order spatial moment along the x direction, in terms of the generating parameters, is given as follows,

$$\langle x^2\rangle_{\mathrm{eLG}} = \frac{\pi\omega_0^4 \exp\left(\frac{\mu_1\mu_2}{2-\eta_1-\eta_2}\right)}{4\mathcal{N}^2_{\mathrm{eLG}}\left(\eta_1+\eta_2-2\right)^3}\left\{\left(\mu_2^2-2\eta_2+2\right)\eta_1^2\right. \tag{31}$$

$$\left. + \left[\left(2\mu_1\mu_2+8\right)\eta_2 - 2\mu_1\mu_2 - 2\mu_2^2 - 2\eta_2^2 - 6\right]\eta_1 + \left(\mu_1^2+2\right)\eta_2^2 - \left(2\mu_1^2+2\mu_1\mu_2+6\right)\eta_2 + \mu_1^2 + 2\mu_1\mu_2 + \mu_2^2 + 4\right\}.$$

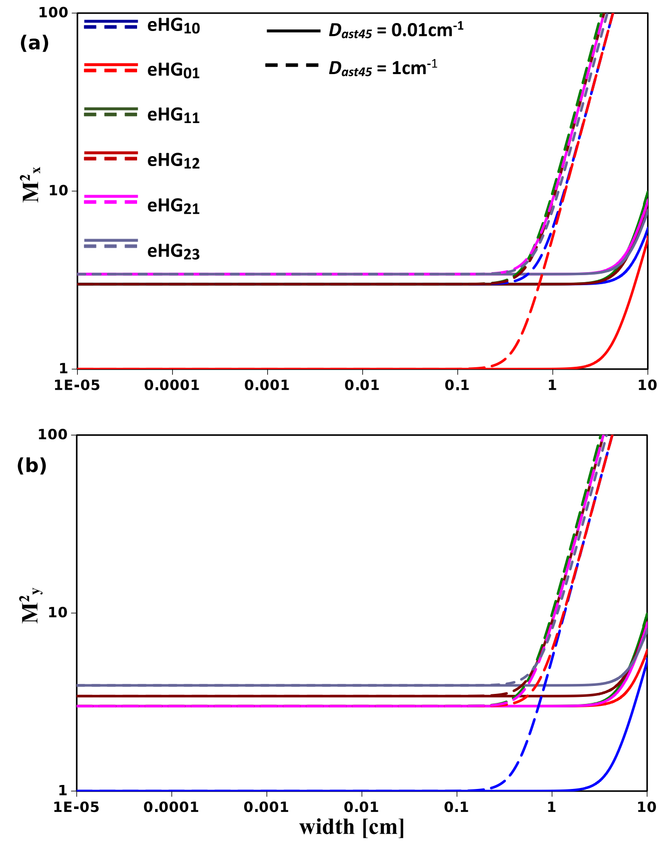

Fig. 3. Beam propagation factor due to 45° astigmatism as a function of beam radius. The solid lines represent the beam propagation factor due to an aberration coefficient of 0.01 cm^{-1} and the dashed lines represent an aberration coefficient of 1 cm^{-1}. The same color is used for both types of lines to represent the same laser beam. (a) shows the beam propagation factor along the x direction, and (b) shows the beam propagation factor along the y direction.

For the second-order angular momentum, the terms in Eq. (18) are given as,

$$\theta_1^{\mathrm{ast45}} = \frac{\exp\left(\frac{\mu_1\mu_2}{2-\eta_1-\eta_2}\right)\left[\mu_1^2 - 2\mu_1\mu_2 + \mu_2^2 + 2\eta_1 + 2\eta_2 - 4\right]}{\pi\mathcal{N}^2_{\mathrm{eLG}}\left(\eta_1+\eta_2-2\right)^3}. \tag{32}$$

where the aberration dependent terms for 45° astigmatism are expressible as follows,

$$\theta_2^{\mathrm{ast45}} = \frac{D^2_{\mathrm{ast45}}\omega_0^4\pi\exp\left(\frac{\mu_1\mu_2}{2-\eta_1-\eta_2}\right)}{4\mathcal{N}^2_{\mathrm{eLG}}\left(\eta_1+\eta_2-2\right)^3\lambda^2}\times\left\{\left(\mu_2^2+2\eta_2-2\right)\eta_1^2 + \left[2\eta_2^2 + \left(-2\mu_1\mu_2-8\right)\eta_2 + 2\mu_1\mu_2 - 2\mu_2^2 + 6\right]\eta_1 + \left(\mu_1^2-2\right)\eta_2^2 + \left(2\mu_1\mu_2 - 2\mu_1^2 + 6\right)\eta_2 + \left(\mu_1-\mu_2+2\right)\times\left(\mu_1-\mu_2-2\right)\right\}, \tag{33}$$

and

$$\theta_3^{\mathrm{ast45}} = \frac{D_{\mathrm{ast45}}\omega_0^3\pi\exp\left(\frac{\mu_1\mu_2}{2-\eta_2-\eta_1}\right)\left[\eta_2\mu_1 - \eta_1\mu_2 + \mu_2 - \mu_1\right]}{2i\mathcal{N}^2_{\mathrm{eLG}}\left(\eta_1+\eta_2-2\right)^2\lambda}. \tag{34}$$

The first-order spatial-angular moment for 45° astigmatism in terms of generating parameters is given as,

$\langle x\theta_x\rangle^{\mathrm{ast45}}$

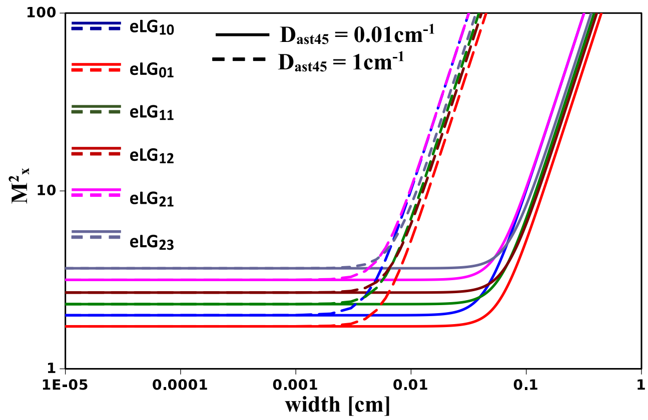

Fig. 4. Beam propagation factor due to 45° astigmatism as a function of beam radius. The solid lines represent the beam propagation factor due to an aberration coefficient of 0.01 cm^{-1} and the dashed lines represent an aberration coefficient of 1 cm^{-1}. The same color is used for both types of lines to represent the same laser beam.

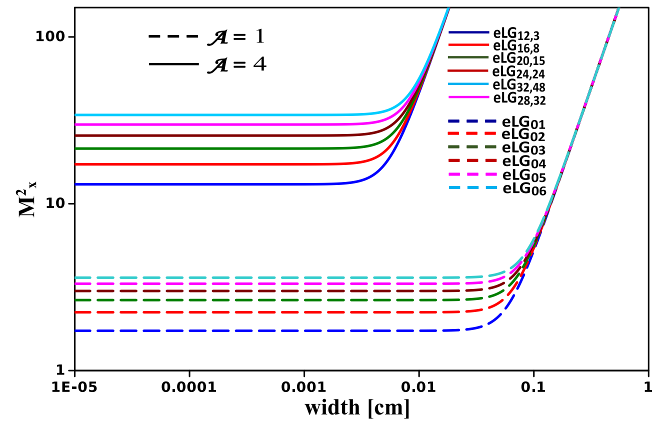

Fig. 5. Beam propagation factor due to 45° astigmatism as a function of beam radius. The dashed lines represent the beam propagation factor when the mode parameter is given by $\mathcal{A} = 1$ and the solid lines represent the mode parameter given by $\mathcal{A} = 4$.

$$= \frac{D_{\text{ast45}}\omega_0^4\pi \exp\left(\frac{\mu_1\mu_2}{2-\eta_1-\eta_2}\right)\left[\left(\eta_1\mu_2+\eta_2\mu_1-\mu_1-\mu_2\right)\left(\eta_1\mu_2-\eta_2\mu_1+\mu_1-\mu_2\right)\right]}{4\mathcal{N}_{\text{eLG}}^2\left(\eta_1+\eta_2-2\right)^3\lambda}. \tag{35}$$

Substitution of Eqs. (33) and (34) into Eq. (18), and subsequent substitution into Eq. (11) together with Eqs. (35) and (32) yields the analytical expression of the beam propagation factor due to 45° astigmatism. The final result is given as follows,

$$M_x^4 = \left(\frac{|\ell|^2+|\ell|+2p}{2p+|\ell|}\right)\left[\frac{\pi^2 D_{\text{ast45}}^2\omega_0^4}{\lambda^2}\left(\frac{|\ell|^2+|\ell|+2p}{2p+|\ell|}\right)+(2p+|\ell|+1)\right], \tag{36}$$

Fig. 4 shows the beam propagation factor of various eLG laser beams aberrated by 45° astigmatism as a function of beam radius.

The solid lines represent the propagation factor of the laser beam due to an aberration coefficient of 0.01 cm^{-1} and the dashed lines represent an aberration coefficient of 1 cm^{-1}. The plots in Fig. 4 have a similar trend: the beam propagation factor is almost flat and changes infinitesimally up until a certain thresh-hold beam radius. As in the case of eHg laser beams, we use the critical width to partition the two regions for eLG laser beams. The critical width is given as,

$$\omega_c^{\text{ast45}} = \sqrt{\frac{\lambda}{\pi D_{\text{ast}}}\left(\frac{2p+|\ell|}{|\ell|^2+|\ell|+2p}\right)}. \tag{37}$$

In the region where the beam radius is larger than the critical width, $\omega_c \ll \omega_0$, the beam propagation factor can be approximated as a quadratic function in beam radius, ω_0,

$$M_x^2 \simeq \frac{\pi\omega_0^2 D_{\text{ast45}}}{\lambda}\left(\frac{|\ell|^2+|\ell|+2p}{2p+|\ell|}\right). \tag{38}$$

Fig. 4 is a log–log plot of the beam propagation factor versus beam radius, therefore Eq. (38) appears as a straight line with a slope determined by the exponent of ω_0 and the y−intercept, for a fixed wavelength, is determined by the azimuthal index, radial index, and the strength of the 45° astigmatism. The beam propagation factor plots for different eLG laser beams cross each other due to the different critical widths. Some eLG beams pass their critical width while others have not and thus move into the region which is described by the straight line while the rest are still relatively flat. However, once all the beams pass their critical width, all the lines remain parallel.

Fig. 5 shows plots for the cases where the beam propagation factor of eLG beams is equal in the region of sharp increase. Here, it can be seen that there exists a set of eLG beams that behave the same under astigmatism. That is, for some constant $\mathcal{A} \geq 1$ which we call the index parameter, there exists a radial index,

$$p > \frac{\mathcal{A}-1}{8}, \tag{39}$$

and an azimuthal index,

$$|\ell| = \frac{\mathcal{A}-1}{2} + \frac{\sqrt{(\mathcal{A}-1)(8p+\mathcal{A}-1)}}{2} \tag{40}$$

which describe eLG beams that have the same beam propagation factor. The case when $\mathcal{A} = 1$ is an interesting case. Here, the azimuthal index is zero, and all the radial modes are in this set. The dashed lines in Fig. 5 represent this case. The solid lines represent the case when $\mathcal{A} = 4$.

4. Numerical simulation

The beam propagation simulation is performed using the angular spectrum method. First, we generate the angular spectrum by computing the Fourier transform of the input function as follows,

$$F(a,b) = \iint u(x,y)\exp\left(-2\pi i\left[ax+by\right]\right)dx\,dy. \tag{41}$$

This is subsequently followed by multiplication of the angular spectrum with the propagation phase factor which is given by,

$$\Phi(a,b) = \exp\left(-2\pi i z\sqrt{a^2-b^2-\frac{1}{\lambda^2}}\right). \tag{42}$$

Finally, to obtain the laser beam at the specified z position, an inverse Fourier transform is performed to give the propagated laser beam,

$$u(x,y,z) = \iint F(a,b)\Phi(a,b)\exp\left(2\pi i\left[ax+by\right]\right)da\,db. \tag{43}$$

To obtain the beam propagation factor, we use the method proposed by Siegman [21]. This method is based on the measurement of the beam width along the propagation axis, and the final result is plotted and compared to the equation,

$$\omega^2(z) = \left(\frac{M^2\lambda}{\pi\omega_0}\right)^2 z^2 - 2z_0\left(\frac{M^2\lambda}{\pi\omega_0}\right)^2 z + \left(\frac{M^2\lambda}{\pi\omega_0}\right)^2 z_0^2 + \omega_0^2. \tag{44}$$

The data is fitted with a quadratic polynomial of the form

$$Y = Az^2 + Bz + C. \tag{45}$$

Upon fitting the polynomial and extracting the pertinent coefficients, the beam propagation factor is calculated as follows,

$$M^2 = \frac{\pi}{\lambda}\sqrt{AC - \frac{B^2}{4}}, \tag{46}$$

Table 2
Critical width of the eHG beams in Figs. 6 and 7 for the highest aberration strength $D_{ast45} = 0.001\ cm^{-1}$.

eHG laser beam	Critical width (cm)
eHG_{10}	0.11
eHG_{01}	0.11
eHG_{11}	0.08
eHG_{23}	0.09

where,

$$A = \left(\frac{M^2\lambda}{\pi\omega_0}\right)^2, \tag{47}$$

$$B = -2z_0\left(\frac{M^2\lambda}{\pi\omega_0}\right)^2, \tag{48}$$

$$C = \left(\frac{M^2\lambda}{\pi\omega_0}\right)^2 z_0^2 + \omega_0^2. \tag{49}$$

5. Results and discussion

The numerical simulation method described in the previous section, Section 4, is used here to validate the analytical results obtained in Section 3. All the results are generated with $\lambda = 680$ nm and the aberration strength considered is in the range $[-0.001\ cm^{-1}, 0.001\ cm^{-1}]$. The numerical simulation is performed with $N_x = 2048$ and $N_y = 2048$, where N_x and N_y are the number of points in the x and y directions, respectively.

5.1. Elegant Hermite-Gaussian beams

Fig. 6 shows the comparison of the beam propagation factor expressions in Eqs. (27) and (28) with numerical simulations. The selected eHG beams have a beam radius $\omega_0 = 0.05$ cm and are subjected to 45° astigmatism. Fig. 6(a) shows M_x^2 plots of selected eHG beams and Fig. 6(b) shows M_y^2 plots of the same eHG beams. It can be seen that the effect of 45° astigmatism is infinitesimal at this beam width for the aberration strength range. The beam propagation factor of the selected eHG beams is practically unchanged. Table 2 shows the critical widths of the selected beams in Fig. 6 calculated at the highest aberration strength ($D_{ast45} = 0.001\ cm^{-1}$). The critical width in Table 2 is the lowest critical width for the range of aberration strengths. This means that any of the selected eHG beams with a radius that is below this width should experience a negligible change in the beam propagation factor. The results in Fig. 6 confirm the latter point since all the plots are flat lines indicating that the beam propagation factor remains unchanged. Fig. 7 also shows the comparison of the beam propagation factor expressions in Eqs. (27) and (28) with numerical simulations, albeit the selected eHG beams have a beam radius $\omega_0 = 0.3$ cm. Here, the effect of 45° astigmatism on the beam propagation factor is clearly discernible for both M_x^2 and M_y^2. The beam radius for the eHG beams in Fig. 7 is larger than the critical width at the aberration strength $D_{ast45} = 0.001\ cm^{-1}$. Therefore, it is expected that the beam propagation factor should deviate from the aberration-free one for all the selected eHG beams. Lastly, the asymmetry in the beam propagation factor along the x and y is easy to see in both Figs. 6 and 7. The laser beam with the lowest beam propagation factor along the x is eHG_{01} whereas the beam with the lowest beam propagation factor along the y is the beam eHG_{10}. Furthermore, the minimum value of M_y^2 for the beam eHG_{23} is larger than the minimum value of M_x^2. This can be seen by taking the values of M_x^2 and M_y^2 for the beam eHG_{11} as the reference since it has the same beam propagation factor in both x and y directions. In all the plots, there is excellent agreement between the numerical results and the analytical results.

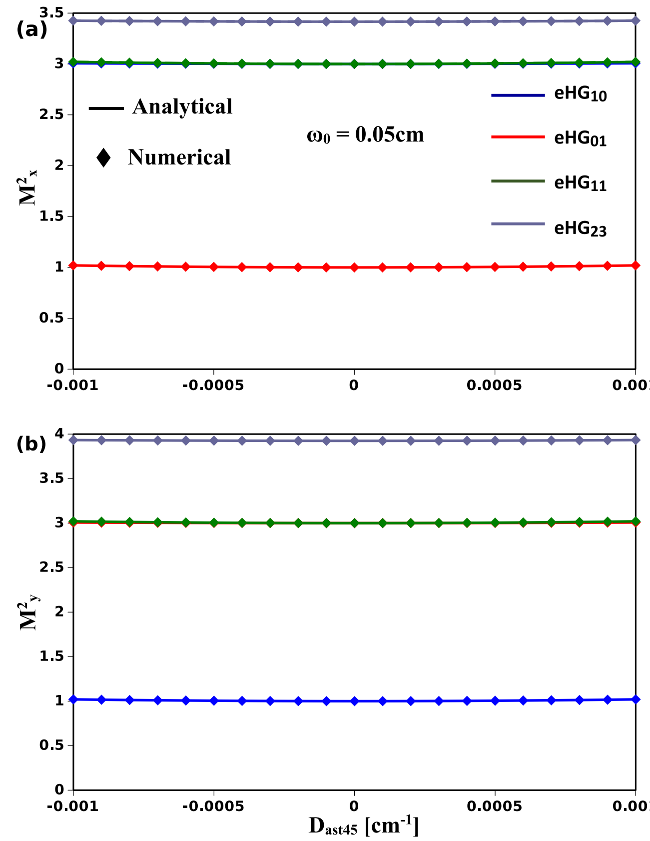

Fig. 6. Beam propagation factor as a function of the 45° astigmatism for various eHG beams. The plots show results for the eHG beams with $\omega_0 = 0.05$ cm; (a) the beam propagation factor along x, (b) the beam propagation factor along y. The solid lines represent the analytical prediction of the beam propagation factor. The discrete markers represent the results of the numerical simulation.

Table 3
Critical width of the eLG beams in Fig. 8 for the highest aberration strength $D_{ast45} = 0.001\ cm^{-1}$.

eLG laser beam	Critical width (cm)
eLG_{10}	0.10
eLG_{01}	0.15
eLG_{11}	0.13
eLG_{23}	0.12

5.2. Elegant Laguerre-Gaussian beams

Fig. 8 shows a comparison of the beam propagation factor expression in Eq. (36) with numerical simulations. It shows two scenarios: Fig. 8(a) shows the beam propagation factor of eLG beams with beam radius $\omega_0 = 0.05$ cm and Fig. 8(b) shows the comparison for eLG beams with beam radius $\omega_0 = 0.3$ cm. Table 3 shows the critical widths of the selected laser beams in Fig. 8 calculated at the highest aberration strength ($D_{ast45} = 0.001\ cm^{-1}$). It can be seen that the beam radius considered in Fig. 8(a) is below the critical width for all the selected eLG beams. Therefore, as expected, the results of the beam propagation factor show no change for all the aberration strengths in the chosen range. Conversely, the beam radius of the eLG beams in Fig. 8(b) is larger than all the critical widths that are shown in Table 3. As predicted in Section 3, the beam propagation factor deviates from the aberration-free case. In both Fig. 8(a) and (b), the beam propagation factor obtained from the numerical simulations matches the beam propagation factor that is calculated using Eq. (36).

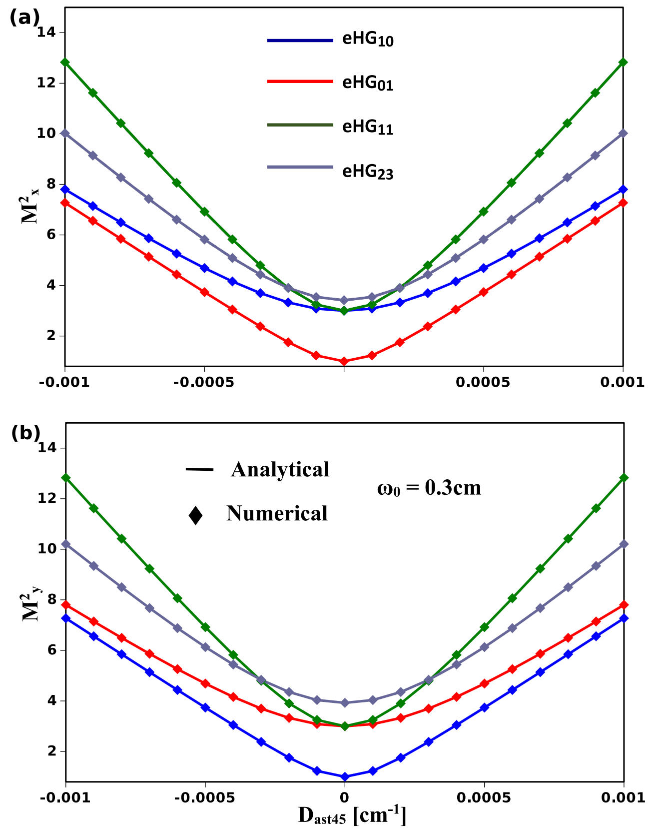

Fig. 7. Beam propagation factor as a function of the 45° astigmatism for various eHG beams. The plots show results for the eHG beams with ω_0 = 0.3 cm; (a) the beam propagation along x, (b) the beam propagation factor along y. The solid lines represent the analytical prediction of the beam propagation factor. The discrete markers represent the results of the numerical simulation.

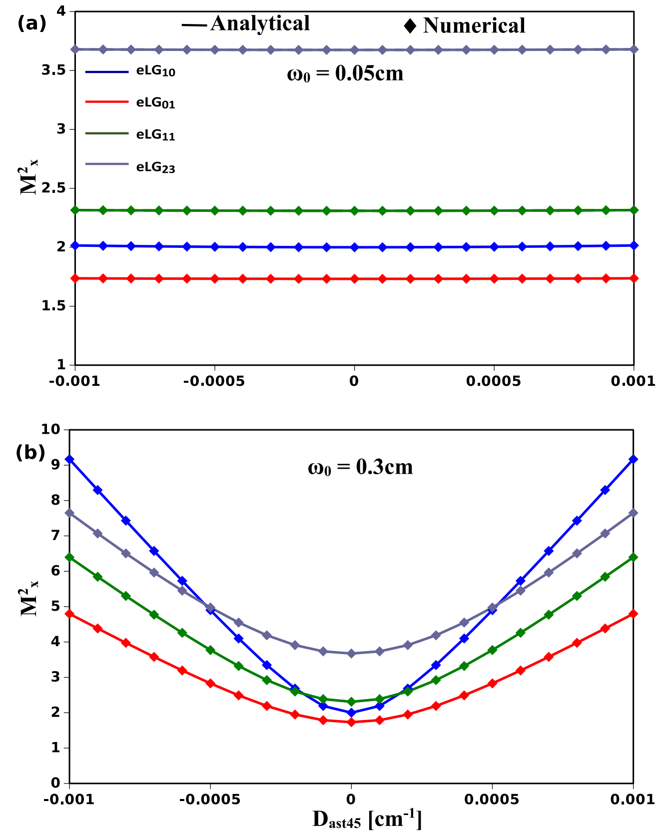

Fig. 8. Beam propagation factor as a function of the 45° astigmatism for various eLG beams. The plots show results for the eLG beams with (a) ω_0 = 0.05 cm; (b) ω_0 = 0.3 cm. The solid lines represent the analytical prediction of the beam propagation factor. The discrete markers represent the results of the numerical simulation.

6. Summary

In this work, we derived compact and simplified analytical expressions for the beam propagation factor of elegant Hermite-Gaussian and elegant Laguerre-Gaussian beams when they are aberrated with astigmatism. Our analytical analysis shows that the effect of astigmatism on the beam propagation factor is not only determined by the astigmatism strength, the beam radius is also a key parameter. As a result, we derived an expression for the beam radius that separates the region where the beam propagation factor is negligibly affected by the presence of astigmatism and the region where it becomes severely affected. We call this the critical width. We found that it is inversely proportional to the strength of astigmatism and also depends on the beam indices. We further derived a limiting expression for the beam propagation factor in the region of sharp increase. The expression shows that the beam propagation factor, within the sharp-growth region, is a quadratic function of beam radius. In the case of the elegant Laguerre-Gaussian beams, we established a parameter that depends on the indices of the elegant Laguerre-Gaussian beams. We call it the index parameter. Based on the index parameter, we further set up expressions that can be used to obtain a set of elegant Laguerre Gaussian beams that have the same beam propagation factor in the region of the sharp increase. The derived analytical expressions for the beam propagation factor were compared with numerical simulations using the angular spectrum method. We found excellent agreement between the analytical results and the numerical simulations. The results of this work contribute to the body of knowledge on elegant Gaussian beams and may be useful in the design of optical systems that are susceptible to astigmatism.

Declaration of competing interest

The authors declare the following financial interests/personal relationships which may be considered as potential competing interests: Chemist Mabena reports financial support was provided by National Research Foundation.

Data availability

Data will be made available on request.

Acknowledgment

The research was carried out with the partial support of a grant from the National Research Foundation (NRF).

References

[1] H. He, N. Heckenberg, H. Rubinsztein-Dunlop, Optical particle trapping with higher-order doughnut beams produced using high efficiency computer generated holograms, J. Modern Opt. 42 (1) (1995) 217–223.

[2] T. Meyrath, F. Schreck, J. Hanssen, C.-S. Chuu, M. Raizen, A high frequency optical trap for atoms using Hermite-Gaussian beams, Opt. Express 13 (8) (2005) 2843–2851.

[3] X.-L. Wang, X.-D. Cai, Z.-E. Su, M.-C. Chen, D. Wu, L. Li, N.-L. Liu, C.-Y. Lu, J.-W. Pan, Quantum teleportation of multiple degrees of freedom of a single photon, Nature 518 (7540) (2015) 516–519.

[4] C.M. Mabena, F.S. Roux, High-dimensional quantum channel estimation using classical light, Phys. Rev. A 96 (5) (2017) 053860.

[5] M.A. Cox, L. Cheng, C. Rosales-Guzmán, A. Forbes, Modal diversity for robust free-space optical communications, Phys. Rev. A 10 (2) (2018) 024020.

[6] R. Fickler, R. Lapkiewicz, W.N. Plick, M. Krenn, C. Schaeff, S. Ramelow, A. Zeilinger, Quantum entanglement of high angular momenta, Science 338 (6107) (2012) 640–643.

[7] Y. Zhang, S. Prabhakar, C. Rosales-Guzmán, F.S. Roux, E. Karimi, A. Forbes, Hong-ou-mandel interference of entangled hermite-gauss modes, Phys. Rev. A 94 (3) (2016) 033855.

[8] I. Nape, B. Sephton, P. Ornelas, C. Moodley, A. Forbes, Quantum structured light in high dimensions, APL Photon. 8 (5) (2023).

[9] S. Saghafi, C. Sheppard, Near field and far field of elegant Hermite-Gaussian and Laguerre-Gaussian modes, J. Modern Opt. 45 (10) (1998) 1999–2009.

[10] S. Saghafi, C. Sheppard, The beam propagation factor for higher order Gaussian beams, Opt. Commun. 153 (4–6) (1998) 207–210.

[11] D. Deng, Q. Guo, L. Wu, X. Yang, Propagation of radially polarized elegant light beams, J. Opt. Soc. Amer. B 24 (3) (2007) 636–643.

[12] S. Luo, B. Lü, Propagation of the kurtosis parameter of elegant Hermite-Gaussian and Laguerre-Gaussian beams passing through ABCD systems, Optik 113 (5) (2002) 227–231.

[13] Z. Mei, D. Zhao, Propagation of Laguerre–Gaussian and elegant Laguerre–Gaussian beams in apertured fractional Hankel transform systems, J. Opt. Soc. Amer. A 21 (12) (2004) 2375–2381.

[14] Z. Mei, The elliptical elegant Laguerre–Gaussian beam and its propagation through aligned and misaligned paraxial optical systems, Optik 118 (8) (2007) 361–366.

[15] W. Nasalski, Elegant Hermite-Gaussian and Laguerre-Gaussian beams at a dielectric interface, Opt. Appl. 40 (2010) 615–622.

[16] J. Qu, Y. Zhong, Z. Cui, Y. Cai, Elegant Laguerre–Gaussian beam in a turbulent atmosphere, Opt. Commun. 283 (14) (2010) 2772–2781.

[17] D. Zhao, Z. Mei, J. Gu, H. Mao, L. Chen, S. Wang, Propagation characteristics of truncated standard and elegant Laguerre-Gaussian beams, in: Adaptive Optics and Applications III, Vol. 5639, SPIE, 2004, pp. 149–158.

[18] Z. Mei, D. Zhao, The generalized beam propagation factor of truncated standard and elegant Laguerre–Gaussian beams, J. Opt. A: Pure Appl. Opt. 6 (11) (2004) 1005.

[19] Z. Mei, D. Zhao, C. Zheng, Analytical expressions of generalized M2 factor of hard-edged diffracted Laguerre–Gaussian beams, Optik 116 (7) (2005) 337–342.

[20] C. Alpmann, C. Schöler, C. Denz, Elegant Gaussian beams for enhanced optical manipulation, Appl. Phys. Lett. 106 (24) (2015) 241102.

[21] A.E. Siegman, New developments in laser resonators, in: Optical Resonators, Vol. 1224, Spie, 1990, pp. 2–14.

[22] A. Siegman, Analysis of laser beam quality degradation caused by quartic phase aberrations, Appl. Opt. 32 (30) (1993) 5893–5901.

[23] T. Johnston, M2 concept characterizes beam quality, Laser Focus World 26 (5) (1990) 173–183.

[24] J.A. Ruff, A. Siegman, Measurement of beam quality degradation due to spherical aberration in a simple lens, Opt. Quantum Electron. 26 (6) (1994) 629–632.

[25] T. Jeong, J. Lee, Accurate determination of the beam quality factor of an AberratedHigh-power laser pulse, J. Korean Phys. Soc. 55 (2) (2009) 488–494.

[26] C. Mafusire, A. Forbes, Generalized beam quality factor of aberrated truncated Gaussian laser beams, J. Opt. Soc. Amer. A 28 (7) (2011) 1372–1378.

[27] J. George, R. Seihgal, S. Oak, S. Mehendale, Beam quality degradation of a higher order transverse mode beam due to spherical aberration of a lens, Appl. Opt. 48 (32) (2009) 6202–6206.

[28] C.M. Mabena, T. Bell, N. Mphuthi, J. Harrison, D. Naidoo, Beam quality factor of aberrated Laguerre-Gaussian optical beams, Opt. Express 31 (16) (2023) 26435–26450.

[29] M.A. Porras, R. Borghi, M. Santarsiero, Relationship between elegant Laguerre–Gauss and Bessel–Gauss beams, J. Opt. Soc. Amer. A 18 (1) (2001) 177–184.

[30] K. Mihoubi, A. Bencheikh, A. Manallah, The beam propagation factor M2 of truncated standard and elegant-Hermite-Gaussian beams, Opt. Laser Technol. 99 (2018) 191–196.

[31] Y. Huang, G. Zhao, Z. Gao, D. He, A comparative study of standard and elegant Hermite–Gaussian beams propagating through turbulent atmosphere, J. Modern Opt. 58 (14) (2011) 1239–1245.

[32] Y. Xu, H. Tian, H. Feng, Q. Du, Y. Dan, Propagation factors of standard and elegant Laguerre Gaussian beams in non-Kolmogorov turbulence, Optik 127 (22) (2016) 10999–11008.

[33] Y. Xu, S. Wang, Z. Zhao, Y. Li, Y. Dan, Comparative studies of properties of standard and elegant Laguerre–Gaussian beams, Optik 127 (5) (2016) 2789–2794.

[34] J. Harrison, W.T. Buono, A. Forbes, D. Naidoo, Aberration-induced vortex splitting in amplified orbital angular momentum beams, Opt. Express 31 (11) (2023) 17593–17608.